

# High resolution speckle sensor for contactless torque measurement in wind energy systems

Jan F. Westerkamp, Michael Sorg, Andreas Fischer

University of Bremen, BIMAQ – Bremen Institute for Metrology, Automation and Quality Science,  
j.westerkamp@bimaq.de

## Abstract:

In order to extend the operating life of drivetrain components of a wind energy system improved data sets of load cycles could greatly enhance the design process. For this purpose, the effects of transient torque reversals which are dependent on the operating conditions as well as the wind characteristics have to be considered. The sensors currently used in condition monitoring systems, however, are mostly inadequate and often limited in access. The proposed optical speckle sensor can measure directly on any shaft material and works contactless, which allows post-installation on existing machines. A concept for an in-situ capable sensor with a resolution of 0.5 % the nominal torque of a generator shaft will be presented and the influence of the compound lens in combination with the image registration algorithm on the resulting measurement uncertainty will be discussed.

**Key words:** wind energy system, torque measurement, speckle sensor, measurement uncertainty

## Introduction

Drivetrains of wind energy systems (WES) suffer a broad range of dynamic loads. Transient torque reversals originate in power loss and emergency stops [1], start cycles [2] and in sheer winds and turbulence [3]. The subsequent failure of bearings and gearboxes result in over 50 % of the downtime of wind energy systems. In order to improve the design of drivetrain components with precise load cycles, additional sensors have to be installed for measuring the torque in shafts with high time resolution.

Compiling load cycle data from supervisory control and data acquisition (SCADA) systems and condition monitoring systems (CMS) is limited because of inadequately measured variables, the missing availability of sensors (especially in older wind energy systems), the limited uncertainty of the possibly installed sensors, and even the access to the datasets because of confidentiality conflicts [4]. Moreover, the drivetrain torque is generally only derived from the electrical output of the generator which usually is limited to the nominal torque and does not record mechanical overload situations. For this reason, a direct measurement approach for acquiring the torque load is required.

## State-of-the-Art

More direct measurements of the actual torque in a wind energy system usually require the

assembly of strain gauges since integrated torque transducers are not a feasible solution, especially for the rotor shaft with torques in the mega newton meter range. However, installing conventional strain gauges is considered to be expensive and difficult [5]. A variety of other sensors and sensor principles have been proposed in order to simplify the application of torque sensors in wind turbines. Magnetostrictive torque sensors have only minimal target requirements, good stability, and like most contactless sensors can withstand overloads [6]. Standard automotive sensors and simple punched metal bands are used to measure angular differences in [7]. This approach still requires some modification of a shaft, and mounting on glass fiber reinforced composites reduced the isolating properties and has acceptance issues because of possible perpendicular loads on such a shaft. Determining the torque from angular differences can be combined with optical capturing of markings applied to a shaft [8]. The sensor described by Menke et al. still requires the modification of the shaft by laser structuring, and thus is difficult to apply as a retrofit package. Directly using images of the shaft surface would obviously result in a sensor capable of measuring angles on all kinds of surfaces and shaft materials. The main requirement, however, is that the surface has discriminable structures and that their movement can be traced down to the nanometer scale. Furthermore, at least a small

section of structure must be unique so it can be used as an index.

### Aim of the paper

This paper discusses a concept for an optical, in-situ capable sensor measuring angular differences without any modifications to the shaft, and calculating the resulting torque based on shaft model.

For this paper the requirements of the sensor are derived from the technical data (Figure 1) of the research wind energy system of the University of Bremen.

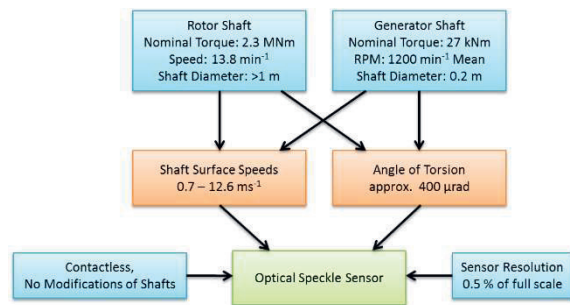


Figure 1: Technical data of the research wind energy system of the University of Bremen, the resulting sensor requirements, and the feasible characteristics of the proposed speckle sensor.

A reasonable choice for the shaft under consideration is the generator shaft due to the fact that its mechanical model is much simpler than that of a typical rotor shaft. For the proof of principle the goal for the torque resolution is defined to 0.5 % (135 Nm) of the nominal torque or full scale for normal sensor operation.

### Measurement principle and experimental setup

The proposed sensor setup depicted in Figure 1, combines two speckle sensors for two angle measurements at the measuring distance  $l = 0.1$  m on the rotor shaft with a radius of  $r = 0.1$  m. With Equation (1) the requirement for the torque ( $M$ ) resolution translates to a surface displacement of  $b = 105$  nm (shear modulus  $G = 82.0$  MNm<sup>-2</sup>).

$$M = \frac{\pi}{2} r^4 G \cdot \frac{\Delta\varphi}{l} \quad (1)$$

$$\Delta\varphi = \frac{1}{r} (b_1 - b_2)$$

Monochromatic speckle patterns emerging from a specific spot of a rough workpiece surface can be regarded as a unique fingerprint of that specific spot [9]. The digital (speckle) image correlation (DIC) has been proposed for strain [10], or surface velocity [11, 12] measurements, and has been used for displacement measurements down to the nanometer scale

[13, 14]. Thus, the requirement for the displacement resolution can be achieved.

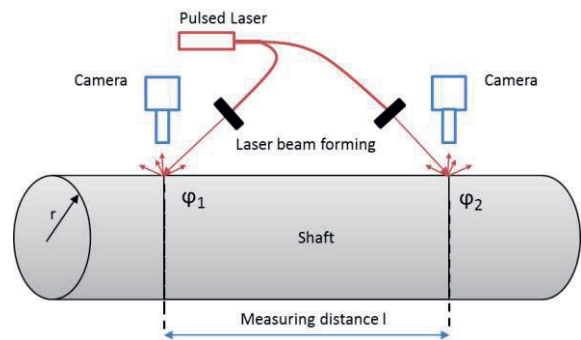


Figure 2: Measurement principle using two synchronized, speckle based angle measuring sensors with a single laser illuminating the surfaces with nano second pulses.

For the proof of principle the experimental setup has been simplified as shown in Figure 3. A target surface is moved ( $x$ -axis) in steps of  $6 \mu\text{m}$  in front of high speed camera with  $1280 \times 1024$  pixels and a pixel size of  $p = 14 \mu\text{m}$ . A capacitive distance sensor is used as reference for the step size. The Laser (not shown) with a wavelength of  $405$  nm illuminates the target surface with a collimator.

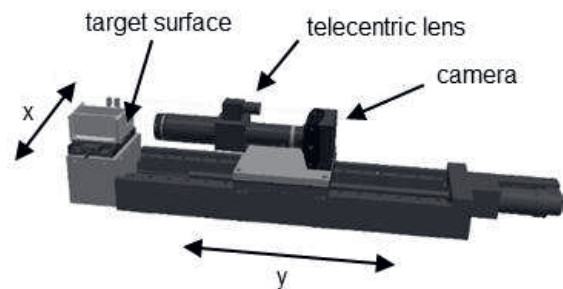


Figure 3: Experimental setup comprising a camera, telecentric lens, a target surface and two linear stages, without the illuminating laser with a wavelength of  $405$  nm.

Vibrations of the WES and subsequently of the torque sensor will result in varying distances between the lenses and the shaft surface. Therefore, the sensor should tolerate small changes with only small effects on the measurement uncertainty. This affects the selection of a suitable lens, which must also have a magnification of 10 to 20 to achieve the required resolution on the camera sensor. For a field mountable sensor system and for having an acute angle between the laser beam and the optical axis of the lens, it is desirable to have a working distance of  $20$  mm to  $100$  mm. In combination with the c-mount adapter of the camera, the lens of choice was a telecentric lens with a magnification of  $m = 10 \pm 5 \%$ , a numerical aperture of  $N.A. = 0.23$  and a working distance of  $WD = 55.3 \pm 2$  mm. Telecentric

lenses are preferable over single-lens systems in most metrological contexts because the relationship between image and object coordinates is straightforward. Additionally, the equations for speckle motion contain fewer parameters than the corresponding equations for a single-lens system [15]. Given the camera pixel size and the magnification the surface displacement resolution of 105 nm equates to a displacement in the image of  $d \approx 0.07$  pixel. The speckle size, as taken from the image, is one pixel.

### Image analysis

There are a number of published approaches for sub-pixel image registration which is required for the targeted resolution. In the current sensor setup the speckle size is too small for typical speckle or PIV image registration algorithms. For this reason the algorithm published by Guizar-Sicairos et al. [17] was used in the experiments. Their efficient algorithm can register images with the same accuracy as the standard FFT approach, and has been classified as the best performing algorithm with realistic images derived from satellite imagery [18]. A recent improvement of this approach by Yousef et al [19] is not considered here, because it is limited to images that differ by small sub-pixel shifts and the performance of the algorithm degrades otherwise.

### Measurement results

The first measurements were carried out with the experimental setup in focus. The precision linear stage with a linear piezo drive in front of the lens was moved 160 times with a step size of  $x = 6.0 \mu\text{m}$  and a picture was taken at each step. A capacitive distance sensor was used as an additional reference for the step size. The images of two adjacent steps were compared with the above mentioned method. The mean displacement was  $\bar{d} = 4.09$  pixel and the experimental standard deviation of the observed values  $s(d) = 0.04$  pixel.

Figure 4 shows the added image displacements translated back into the coordinate system of the linear stage. Using the propagation of uncertainty, the steps of the linear stage could be estimated with an uncertainty of  $u(x) = 54$  nm. The linearity of the measurement was very good (coefficient of determination  $R^2 \approx 1$ ). Using Equation (2) for calculating the combined standard uncertainty [20] of the torque measurement a resolution of 102 Nm, respectively 0.38 % of the nominal torque was achieved.

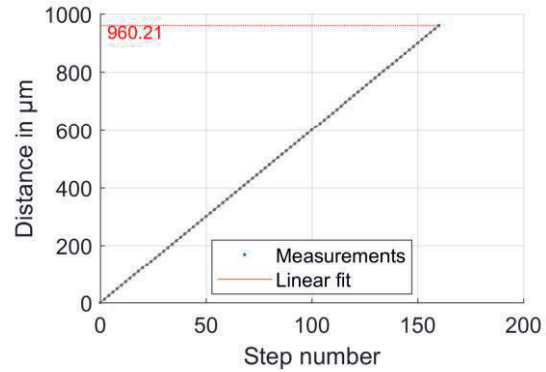


Figure 4: *x*-Displacement of the surface as measured by the optical sensor with only every second step of the 160 steps shown for clarity; linear approximation through all measurements with a coefficient of determination  $R^2 \approx 1$ .

$$u(M) = \sqrt{\left(\frac{\partial M}{\partial d_1}\right)^2 u^2(d_1) + \left(\frac{\partial M}{\partial d_2}\right)^2 u^2(d_2)} \\ = \sqrt{2} r^3 G \frac{p}{l m} u(d) \quad (2)$$

The telecentric lens has the advantage of a constant magnification across the whole depth of field (DOF). Even though the DOF of the lens for this study is only 0.02 mm, the same measurements were repeated with varying working distances by moving the linear stage along the *y*-axis. The experimental standard deviation of the mean of the steps in *x*-direction was used to calculate the actual magnification of the telecentric lens. The mean value of the magnification at the focus distance was  $\bar{m} = 9.54$  with a combined standard uncertainty of  $u(\bar{m}) = 0.02$  with a coverage factor of  $k = 2$ .

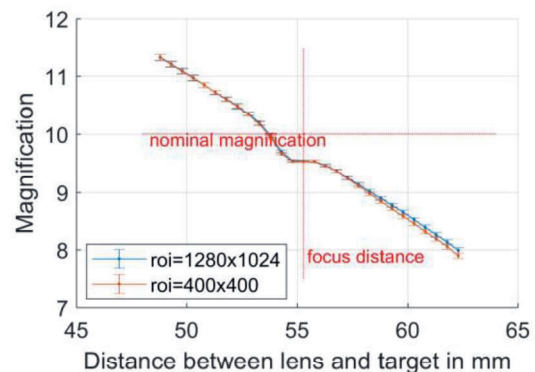


Figure 5: Magnification of the telecentric lens as a function of the distance between lens and target surface. The usable working distance is larger than the depth of field of 0.02 mm. Two different regions of interest (roi) for the image registration were evaluated.

As shown in Figure 5 the magnification remains practically constant ( $\pm 0.5$  mm) around the working distance of the telecentric lens and as expected varies significantly otherwise.

## Conclusions and outlook

The results show that the proposed sensor in this proof of concept configuration is capable of the stipulated resolution of 0.5 % (135 Nm) of the nominal torque with regard to the influences of the sensor setup and the image registration algorithm.

Using speckle patterns and not direct surface characteristics has the effect that a varying distance between lens and shaft has only a small influence on the measurement, at least regarding the influence of the magnification on the displacement measurement. The allowable range increases from  $\pm 0.01$  mm, as expected

from the DOF, to  $\pm 0.5$  mm around the working distance of the telecentric lens.

From Equation (1) it is obvious that several other influences contribute to the uncertainty of a fully developed optical torque sensor. Further research will address some of these issues (see Figure 6) especially on the sensor side, and will be targeted at implementing a sensor comprising two angle measurement units as well a testing on a testbed for dynamic torque measurements at the targeted surface speeds of up to 15 m/s.

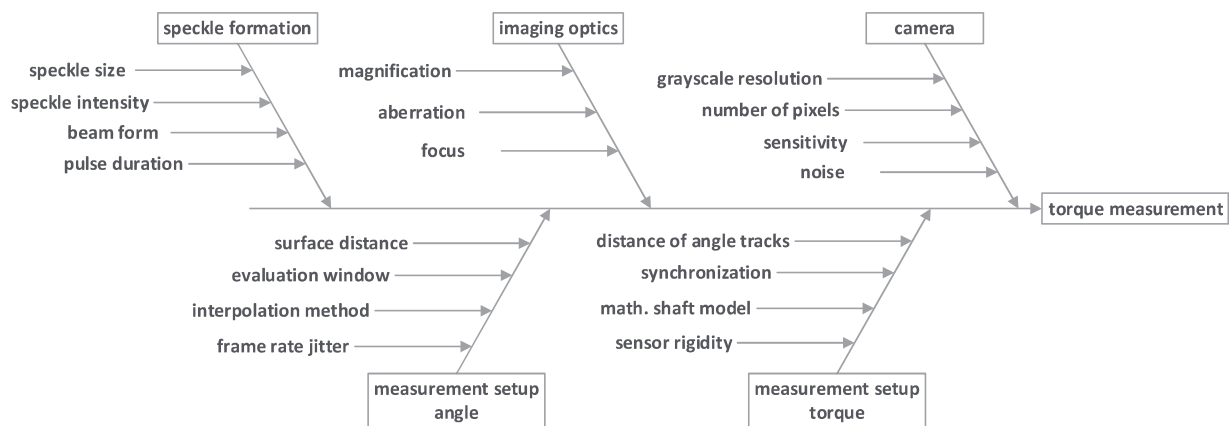


Figure 6: A subset of influences on the uncertainty of the torque measurement.

## References

- [1] A. Greco, S. Sheng, J. Keller, and A. Erdemir, Material wear and fatigue in wind turbine Systems, *Wear*, vol. 302, no. 1–2, pp. 1583–1591 (2013); doi: 10.1016/j.wear.2013.01.060
- [2] J. Rosinski and D. Smurthwaite, Troubleshooting wind gearbox problems, *Gear Solutions*, vol. 8, pp. 22–33 (2010)
- [3] D. Herr and D. Heidenreich, How turbulent winds abuse wind turbine drivetrains, *Windpower Engineering & Development*, vol. 7, no. 2, p. 41f (2015)
- [4] Y. Feng, Y. Qiu, C. J. Crabtree, H. Long, and P. J. Tavner, Monitoring wind turbine gearboxes, *Wind Energy*, vol. 16, no. 5, pp. 728–740 (2013); doi: 10.1002/we.1521
- [5] B. Lu, Y. Li, X. Wu, and Z. Yang, A review of recent advances in wind turbine condition monitoring and fault diagnosis, in 2009 IEEE Power Electronics and Machines in Wind Applications, (2009), pp. 1–7, ; doi: 10.1109/PEMWA.2009.5208325
- [6] F. T. Calkins, A. B. Flatau, and M. J. Dapino, Overview of Magnetostrictive Sensor Technology, *Journal of Intelligent Material Systems and Structures*, vol. 18, no. 10, pp. 1057–1066 (2007); doi: 10.1177/1045389X06072358
- [7] A. Vath, B. R. AG, and S. Grimm, Reliability and Energy Yield Increase of Wind Turbines as a Benefit of Dynamic Load Reduction Operation, in EWEA Europe's Premier Wind Energy Event, (2014)
- [8] T. Menke, C. Unger, A. Dai, D. Kramer, B. Eilert, G. Ullmann, and L. Overmeyer, Development of a Combined Measurement System for Torque and Angular Position, *Procedia Technology*, vol. 26, pp. 136–143 (2016); doi: 10.1016/j.protcy.2016.08.019
- [9] G. Goch, H. Prekel, S. Patzelt, M. Faravashi, and F. Horn, Precise Alignment of Workpieces Using Speckle Patterns as Optical Fingerprints, *CIRP Annals - Manufacturing Technology*, vol. 54, no. 1, pp. 523–526 (2005); doi: 10.1016/S0007-8506(07)60160-7
- [10] D. Amodio, G. B. Broggiato, F. Campana, and G. M. Newaz, Digital speckle correlation for strain measurement by image analysis, *Experimental Mechanics*, vol. 43, no. 4, pp. 396–402 (2003); doi: 10.1007/BF02411344

- [11] B. Ruth, Velocity measurement by the laser speckle method using optical fibres, *Optics & Laser Technology*, vol. 19, no. 2, pp. 83–90 (1987); doi: 10.1016/0030-3992(87)90024-7
- [12] H. Fujii, T. Asakura, and T. Okamoto, Detection properties of an optical fiber probe for laser speckle velocimetry, *Optics Communications*, vol. 55, no. 6, pp. 393–398 (1985); doi: 10.1016/0030-4018(85)90138-5
- [13] A. Tausendfreund, D. Stöbener, G. Dumstorff, M. Sarma, C. Heinzl, W. Lang, and G. Goch, Systems for locally resolved measurements of physical loads in manufacturing processes, vol. 64, no. 1, pp. 495–498, ; doi: 10.1016/j.cirp.2015.03.005
- [14] B. Pan, K. Qian, H. Xie, and A. Asundi, Two-dimensional digital image correlation for in-plane displacement and strain measurement: a review, *Measurement Science and Technology*, vol. 20, no. 6, p. 062001 (Apr. 2009); doi: 10.1088/0957-0233/20/6/062001
- [15] P. K. Rastogi, Ed., *Digital Speckle Pattern Interferometry and Related Techniques*. John Wiley & Sons Inc, (2001)
- [16] J. C. Dainty, Ed., *Laser Speckle and Related Phenomena (Topics in Applied Physics)*. Springer, (1984)
- [17] M. Guizar-Sicairos, S. T. Thurman, and J. R. Fienup, Efficient subpixel image registration algorithms, *Optical Letters*, vol. 33, no. 2, pp. 156–158 (2008); doi: 10.1364/OL.33.000156
- [18] R. A. Reed, *Comparison of subpixel phase correlation methods for image registration*. Aerospace Testing Alliance, Arnold AFB, TN, USA, 2010
- [19] A. Yousef, J. Li, and M. Karim, High-Speed Image Registration Algorithm with Subpixel Accuracy, *IEEE Signal Processing Letters*, vol. 22, no. 10, pp. 1796–1800; doi: 10.1109/LSP.2015.2437881
- [20] Joint Committee for Guides in Metrology, *Evaluation of Measurement Data - Guide to the Expression of Uncertainty in Measurement*, JCGM 100:2008